Direct visualization of evanescent optical waves

Dimitri A. Papathanassoglou[a)]
Department of Physics, Section of Astrophysics, Astronomy and Mechanics, University of Athens, Panepistimioupolis, 15784 Zografos, Athens, Greece

Brian Vohnsen
Laboratorio de Optica (Departamento de Fisica), Campus de Espinardo (Edificio C), Universidad de Murcia, 30071 Murcia, Spain

(Received 3 September 2002; accepted 11 February 2003)

The existence of evanescent optical waves is usually demonstrated by the observation of transmitted light in frustrated total-internal-reflection experiments that make use of two closely spaced prisms. The main characteristic of a monochromatic evanescent plane wave is the exponential decay of its amplitude in the direction perpendicular to its surface of generation. This decay, however, is not what is seen in the usual experiments when the gap between the prisms is small. Only when the gap is sufficiently large does it gradually approach the exponential dependence. We use a different technique that uses a local probe to reveal the presence of an evanescent wave. The results come closer to the ideal of the exponential decay of the wave amplitude, and the presence of the evanescent wave can be seen directly, making it a suitable demonstration for pedagogical purposes.

[DOI: 10.1119/1.1564811]

I. INTRODUCTION

It may be argued that the existence of evanescent optical waves was first demonstrated in the work on frustrated total internal reflection by Isaac Newton,[1] even though he strongly opposed the notion of waves in optics. With the technique used by Newton it became possible to observe the transmission of light across a narrow gap that separates two plane-parallel surfaces of dielectric media (prisms) when a beam of light is incident at an angle that exceeds the critical angle in the first medium. The reason why the term frustrated is used is that the light will be totally internally reflected at the first interface, and no light will be transmitted to the observer, unless a second medium is present in the vicinity of the first one. Thus, the presence of the second medium is necessary to reveal the presence of the evanescent wave field.

Many experiments have been performed to examine the transmission properties of frustrated total internal reflection (see Refs. 2–5), including its dependence on the angle of incidence, polarization, gap width, and the refractive indices of the three-layered structure. Initially, some confusion appears to have existed as to the suitable definition of an unambiguous penetration depth of the evanescent wave field. It was determined by gradually increasing the gap width until no transmitted light could be visually observed, and it was therefore concluded that the penetration depth depended on the polarization[2] and intensity[2,4] of the incoming light. Eventually, a proper theoretical analysis[4] led to a simpler definition of a penetration depth without contradicting the already established results.

A common feature of most frustrated total internal reflection experiments is that the intervening gap is exceedingly narrow (typically only a fraction of the wavelength) in order to assure a relatively large transmission efficiency. In this case, however, the intensity of the transmitted light does not display a simple exponential dependence on the gap width. Obviously, the presence of the second medium alters the configuration to such a degree that the experiment does not merely illustrate the presence of a single evanescent wave in the gap. This simplification only becomes approximately valid as the gap width is further increased which, in our opinion, makes frustrated total internal reflection a less useful candidate for demonstrating the properties of evanescent waves. To obtain a simple exponential distance dependence, we should ideally do away with the second medium and try to access the generated evanescent wave in a more passive manner. Hall[4] saw no way to reduce the influence of the second medium on the field distribution, and thereby verify his predictions for a single evanescent wave at optical wavelengths, although he did demonstrate that a field was present beyond the boundary of total internal reflection. Other authors[6] have confirmed the presence of this field by use of absorption techniques. Studies aimed at observing the presence of a single evanescent microwave have been realized by use of a local detector probe in order to perturb and thereby modify the evanescent wave field less than with an extended medium as probe.[7] Curiously, these authors wrote that ‘‘this kind of detector probe cannot be imagined at optical wavelengths.’’ Such a probe of evanescent optical fields has, however, already been realized with the technique of scanning near-field optical microscopy in the configuration often referred to as a photon scanning tunneling microscope or a scanning tunneling optical microscope.[8,9] Unfortunately, experiments with these kinds of microscopes typically depend on a high level of technical expertise and instrumentation that is probably not readily available to students. On the other hand, it is essential to have physics students become familiar with the concepts of evanescent waves because in recent years there has been a large growth in their applications such as in optical imaging[8–10] and integrated optical components.[11]

In this paper we provide direct experimental evidence of the presence of an evanescent wave by incorporating a local probe to perturb and thereby allow the observation of the field similar to the techniques used with near-field optical microscopy. Our approach also provides sufficiently strong scattering of light to be observed directly by the eye or a

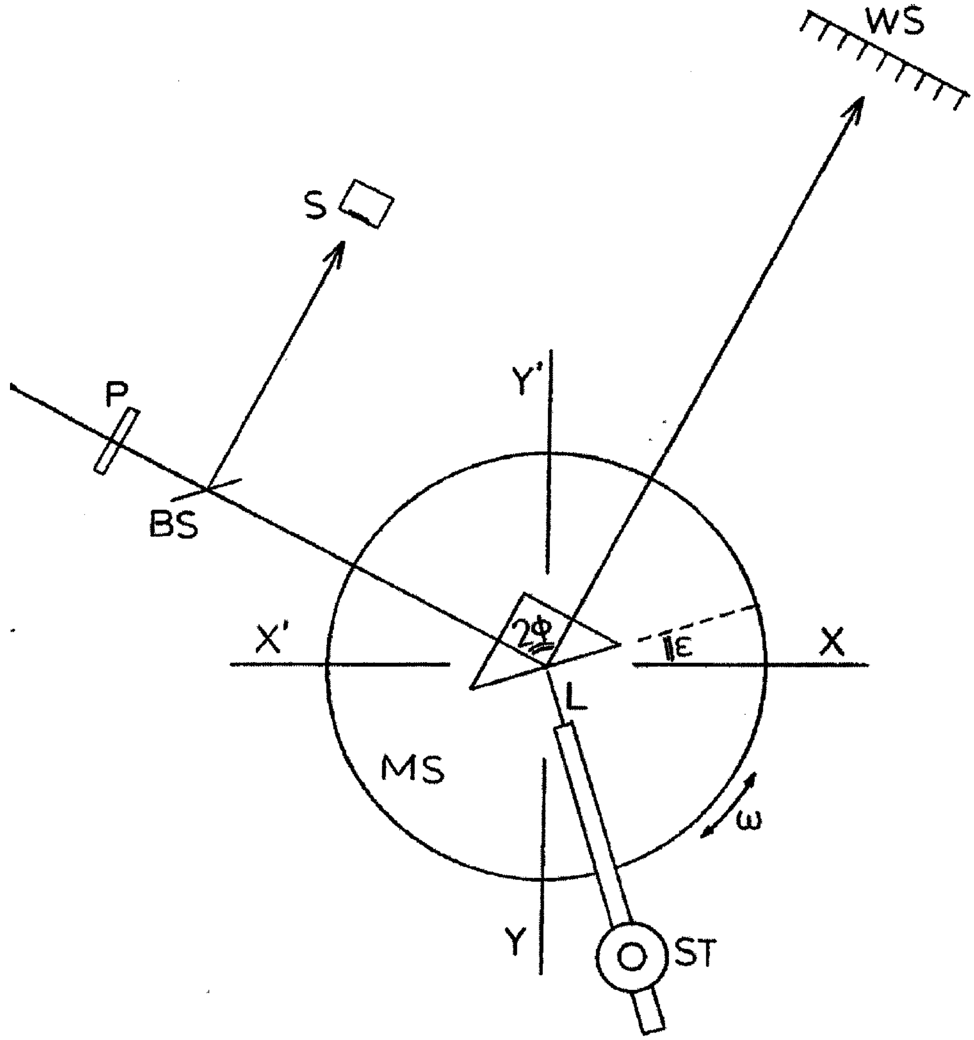

Fig. 1. Schematic of the experimental setup used. P: polarizer, BS: beam splitter, S: sensor of reference beam, MS: circular microscope stage with prism, XX′, YY′: motion axes of the stage, ST: separate stand, L: light probe, ϕ: the angle of incidence, ω: the angle of rotation of the microscope stage, ε: the angle between the prism hypotenuse and the XX′ axis, WS: wall scale for measuring the angle of incidence.

camera. To our knowledge, this type of direct demonstration, suitable for educational purposes, has not been carried out previously.

II. THEORETICAL BACKGROUND

We study the total internal reflection of a beam of light at the inner surface of a prism (see Fig. 1). For simplicity, we do not take account of the finite width of the incident beam, but simply consider the total internal reflection of a monochromatic plane wave at a glass–air interface. Thus, the solution for the field **E** beyond the surface is that of a single evanescent wave as described in most textbooks on optics (excluding its time dependence):[12]

$$\mathbf{E}(x,y)=\mathbf{A}\exp(ikx)\exp(-y/d), \tag{1}$$

where $k=(2\pi/\lambda)n\sin\varphi$ is the component of the wave vector parallel to the interface, λ is the vacuum wavelength of the light, and n is the refractive index of the prism. The vector amplitude of the transmitted field, **A**, depends on the amplitude and the polarization of the incoming field, and the angle of incidence, φ, but only the latter enters into the expression of the field penetration depth, d, defined by

$$d(\varphi)=\frac{\lambda}{2\pi\sqrt{n^2\sin^2\varphi-1}}. \tag{2}$$

The intensity of the evanescent wave is

$$\mathbf{I}(y)=C|\mathbf{A}|^2\exp(-2y/d), \tag{3}$$

where C is a constant for a given polarization.[9,13]

The evanescent wave of Eq. (1) will be probed in our experiment, and we expect our results to agree with the intensity dependence expressed in Eq. (3). Obviously, how accurately our results are in agreement with Eq. (3) depends on how well Eq. (1) expresses the actual field in the system. The presence of a probe or a second prism as in standard frustrated total internal reflection perturbs and thereby modifies the field. We shall make the assumption of a passive probe which has been found to be adequate in many instances of near-field optical microscopy when the sample is a dielectric.[14] This assumption simplifies the theory considerably and is consistent with the experimental results.

III. APPARATUS AND METHOD

The experimental setup is shown in Fig. 1. The linearly

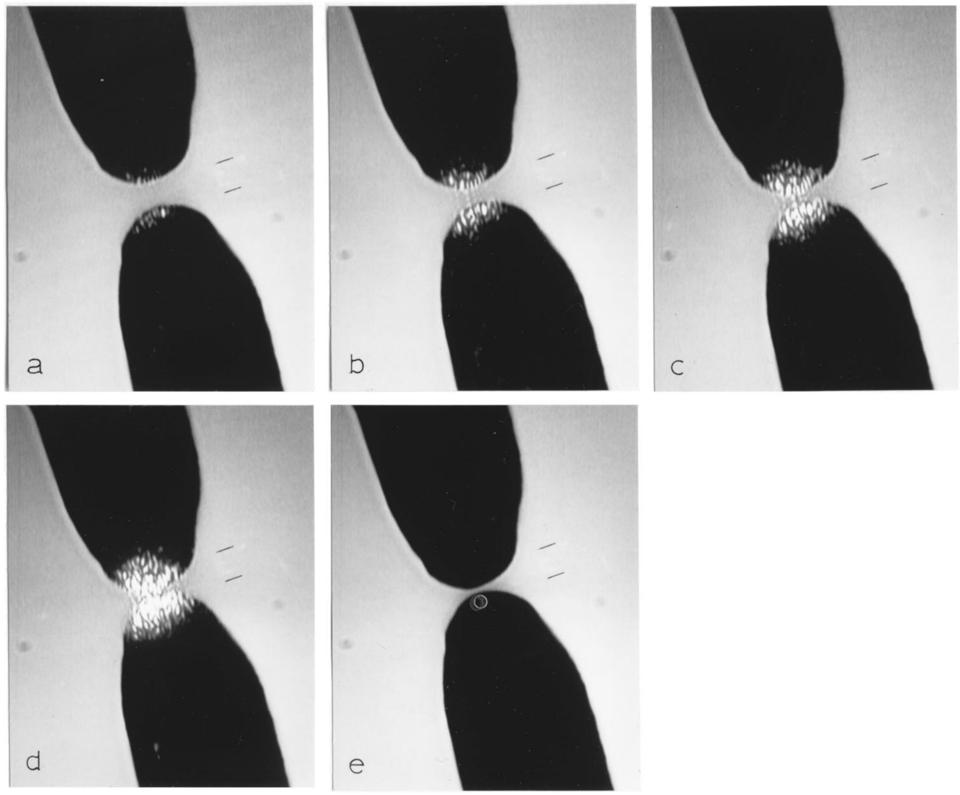

Fig. 2. Microscopic photographs of the scattered light produced by the interaction of the probe with the evanescent wave field. The lower image of the probe is the direct one, while the upper one is produced by reflection at the surface of the prism. The probe-to-surface distance has been decreased gradually in the series of images [(a)–(d)]. Images (d) and (e) have been obtained at the same probe-to-surface distance, but with the laser illumination on and off, respectively. The distance between the two line markers is 10 μm. The small circle in (e) indicates the area imaged on the radiometer sensor used when estimating the intensity of the evanescent wave.

polarized beam from a 10-mW HeNe laser ($\lambda = 0.6328\ \mu$m) is incident on a right angle high quality BK-7 prism ($n = 1.515$) which is fixed on a glass substrate and mounted on the stage of a measuring microscope (Veb Carl Zeiss Jena). The angle of incidence on the hypotenuse face of the prism is chosen to be only slightly larger than the critical angle of $\sim$41.30° to assure a large penetration depth of the evanescent wave, and thereby reduce the demands for accurate positioning equipment. The probe of the evanescent wave is the carefully rounded tip of a thin ($\sim$50 μm) steel wire mounted on a separate stand. This blunt probe ensures a relatively large volume of interaction with the evanescent wave in order to produce sufficient light scattering for our observations, and it is less vulnerable to damage than the narrow fiber tips commonly used in near-field optical microscopy. The position of the prism with respect to the probe is controlled by moving the microscope stage along the x axis at divisions of 3 μm (after modification), along the y axis at divisions of 10 μm, and rotated at divisions of 0.1°. Both the x-axis translation and the rotation have been motorized for accuracy and convenience. Angular increments down to 0.017° are readable by use of the displacement of the spot produced on the opposite room wall by the totally internally reflected beam (Fig. 1). This readable angle on the wall corresponds to an angular resolution of approximately 0.010° for the angle of incidence at the hypotenuse face of the prism. To adjust the probe-to-surface distance, the prism is moved with the stage along the x axis, but inclined at an angle of $\varepsilon = 10°$, so that $\Delta y = \tan(10°)\Delta x \approx 0.176\Delta x$.

To better observe the scattered light produced by the interaction of the probe with the evanescent wave, the microscope was equipped with a 20$\times$ objective (NA$=$0.4 and WD$=$3.3 mm) and a video camera together with a TV monitor (not shown in Fig. 1 for simplicity). Using the conventional under-the-stage illumination, two images of the probe are produced as shown in Fig. 2. One is the direct image, whereas the other image results from reflection on the hypotenuse surface of the prism. Note that even though the prism surface cannot be distinguished in the figure, the simultaneous appearance of two probe images permits an easy measurement of the probe-to-surface distance, y, which is equal to half of the distance between them. When the probe is within a few microns from the surface of the prism, light appears at its apex (see Fig. 2). This is scattered light produced by the perturbation of the evanescent wave by the presence of the probe, and hence it becomes more pronounced as the probe-to-surface distance is decreased further. As expected, the bright areas are composed of interference fringes because of the coherent illumination. We should mention that to avoid extraneous light scattering, great care should be taken to eliminate dust contamination at both the prism and the probe, and it proved necessary for us to clean them several times in the course of the experiments.

Probe-to-surface distance measurements were carried out on the TV monitor during the playback of a video recording. With the distance calibrated by use of a micrometric reticle, the conversion from monitor to object plane was found to be 0.584 μm/mm (corresponding to an overall image magnifi-

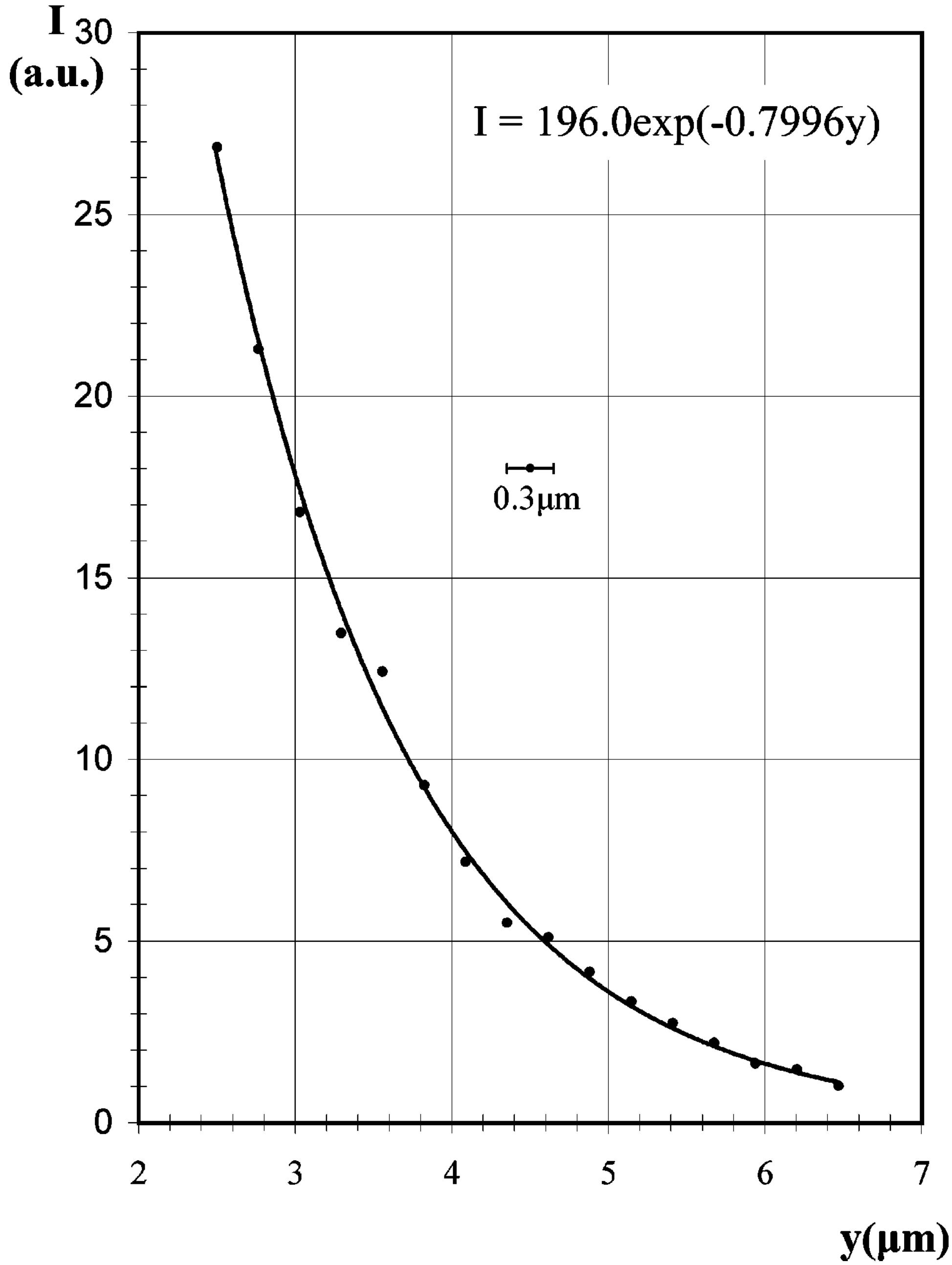

Fig. 3. Intensity of an evanescent wave, *I*, vs the probe-to-surface distance, *y*: measured values (dots) and best theoretical fit (line). The results have been obtained for a fixed angle of incidence $\varphi \approx 41.344°$.

cation of 1712×). Very close to the point of contact between probe and prism ($y < 0.5\ \mu$m), the distance could not be measured in this manner because of the lack of resolution in both the optical and monitored images. In this case we instead used the readings of the *x*-axis motion control. The actual point of contact ($y = 0$) was found with sufficient accuracy by gradually moving the prism toward the probe until a simultaneous lateral displacement of both probe images became noticeable.

To compare the observations with the theoretical predictions for a single evanescent wave, photometric measurements were carried out on the monitored images. We projected (with unit magnification) the direct image of the probe from the TV monitor onto the circular (6.5 mm diam) sensor of a laser radiometer so that it detected a small part of the glowing tip. The photometric measurements were facilitated by the fact that, contrary to the image of the probe produced by reflection, the direct probe image remained steady when the prism underwent translations. The center of the sensor area was displaced 4.25 mm from the apex of the imaged probe corresponding to 2.5 μm in the object plane [Fig. 2(e)]. This quantity was added to the measured values of *y* to obtain the distance between the center of the sensor and the prism face. When this distance is used in the comparison of the measurements with the theoretical predictions, the intensity variation across the sensor must be linear. For the evanescent wave this linearity is only approximately valid, but we found our results to be satisfactory because of the large penetration depth used.

The direct use of the radiometer readings for the intensity

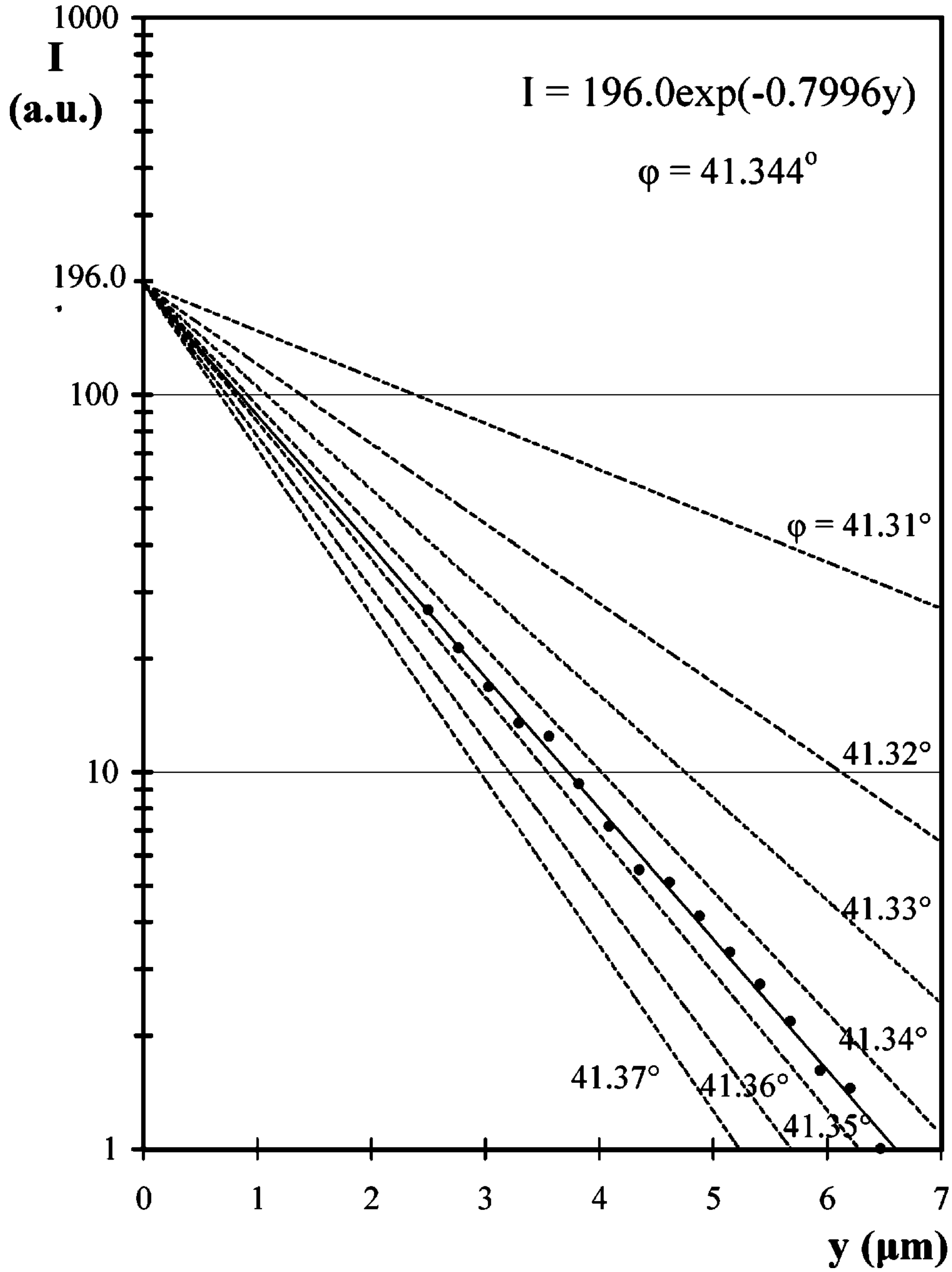

Fig. 4. Same as in Fig. 3 but on a semi-log plot. For comparison, different theoretical lines for other angles of incidence have been shown (dotted lines).

of the evanescent wave was avoided because these were difficult to interpret because of the nonlinearities of the system (gain variations, TV phosphor saturation, blooming of the charge coupled device, etc.). Instead, the following technique, which is free from calibration problems, was applied: For each measurement the intensity of the incident beam was attenuated with a linear polarizer and the TV image dimmed until the radiometer showed a predetermined very low reading, the same in all cases. Another fraction of the incident beam was directed toward a separate sensor (Fig. 1) that measured the relative intensity of the incident beam. With the beam attenuated, the relative intensity was a measure of the attenuation needed for the radiometer to reach the predetermined level. This signal, as can be easily shown, is inversely proportional to the intensity of the evanescent wave before attenuation. By this technique the intensity of the evanescent wave was measured as the inverse of the reading of the separate sensor. To reduce the source of possible noise, the main voltage was stabilized for all apparatus by the use of a voltage stabilizer.

IV. EXPERIMENTAL RESULTS AND DISCUSSION

To examine the correspondence between our measurements and the theoretical predictions for a single evanescent wave in greater detail, we carried out measurements by varying in turn the parameters y and φ. The reason for varying both of these parameters stems from the fact that by the substitution of Eq. (2) into Eq. (3), the intensity $I(y,\varphi)$ of the evanescent wave can be expressed in terms of both y and φ. As mentioned, the angle of incidence was chosen to be only slightly larger than the critical angle in the prism. Thus,

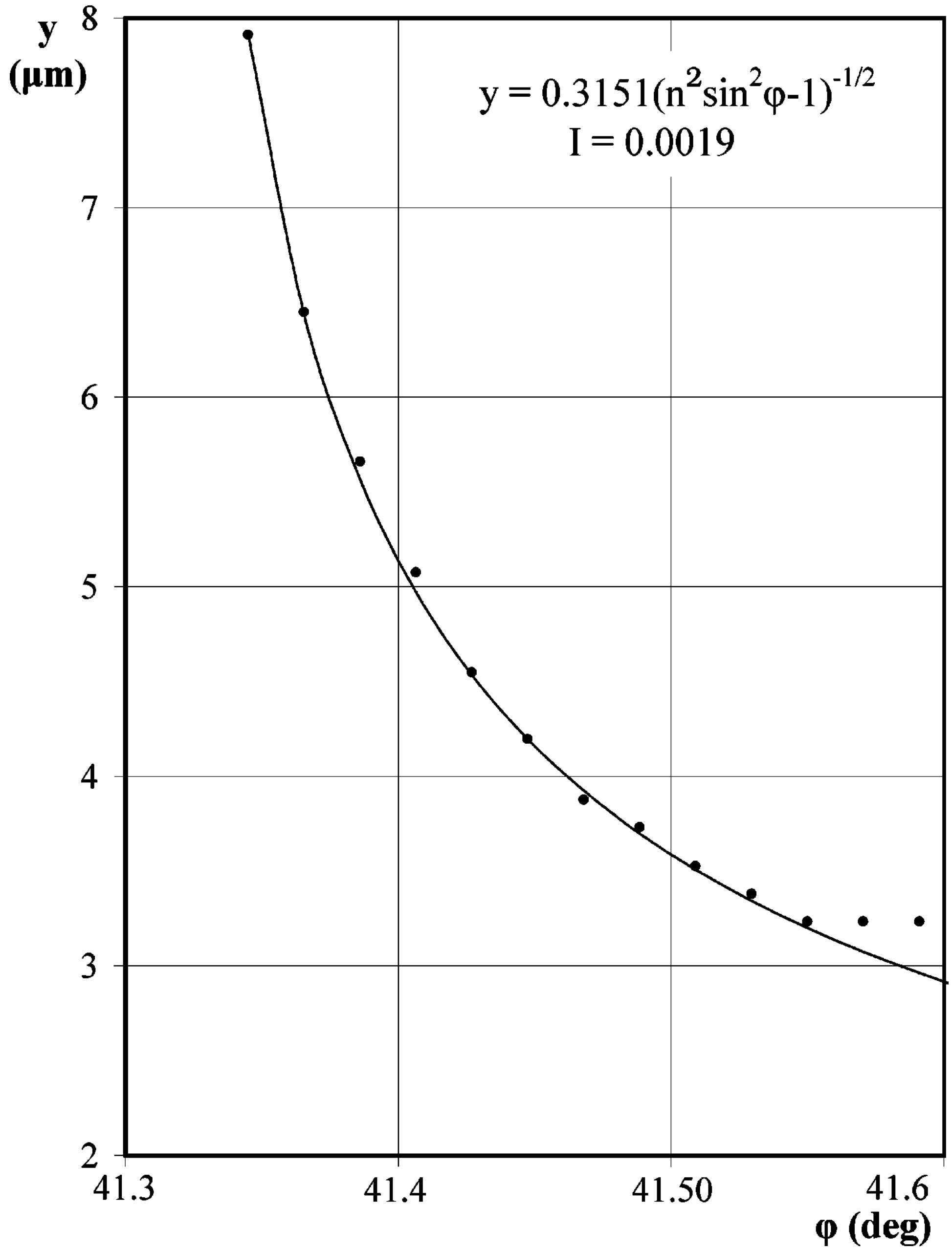

Fig. 5. Probe-to-surface distance vs the angle of incidence for a constant level of intensity. Other details are the same as in Fig. 3.

the smallest allowable angle was dictated by the requirement that all of the incident beam should undergo total internal reflection when not perturbed by the probe. We found that the smallest angle of incidence should be $41.34° \pm 0.01°$ to ensure that neither stray light nor the divergence of the beam (1.2 mrad) should have any noticeable influence on the result. The estimated spread in angle values is mainly a result of inaccurate positioning of the probe within the center of the area illuminated by the beam. This choice of angle corresponds to a maximum penetration depth of $d = (2.78 \pm 0.41)$ μm.

In Fig. 3 measurements of $I(y)$ for the minimum angle of incidence are shown together with a theoretical fit based on Eq. (3) for $\varphi = 41.344°$. The dispersion in the values of y was estimated as ~ 0.30 μm by repeated measurements. The fitted curve corresponds to an evanescent wave with a penetration depth of $d \approx 2.56$ μm, which is within the error range already established. A small undulation appears to be superimposed on the distribution of the measured values, but it is not pronounced enough to reveal its cause. An alternative representation can be obtained in a semi-logarithmic plot in which case the experimentally obtained data should be distributed along a straight line in order to reflect an exponential dependence. This representation is shown in Fig. 4 for the same set of data. For comparison, a number of other lines corresponding to slightly different angles of incidence have also been drawn. The penetration depth of the evanescent wave can be easily determined from the slope of the line.

In the following experiment we tried to maintain a constant level of the measured intensity, I_0, by adjusting in unison the probe-to-surface distance and the angle of incidence. The outcome of this experiment is shown in Fig. 5 together with a theoretical fit based on the (only approximately valid)

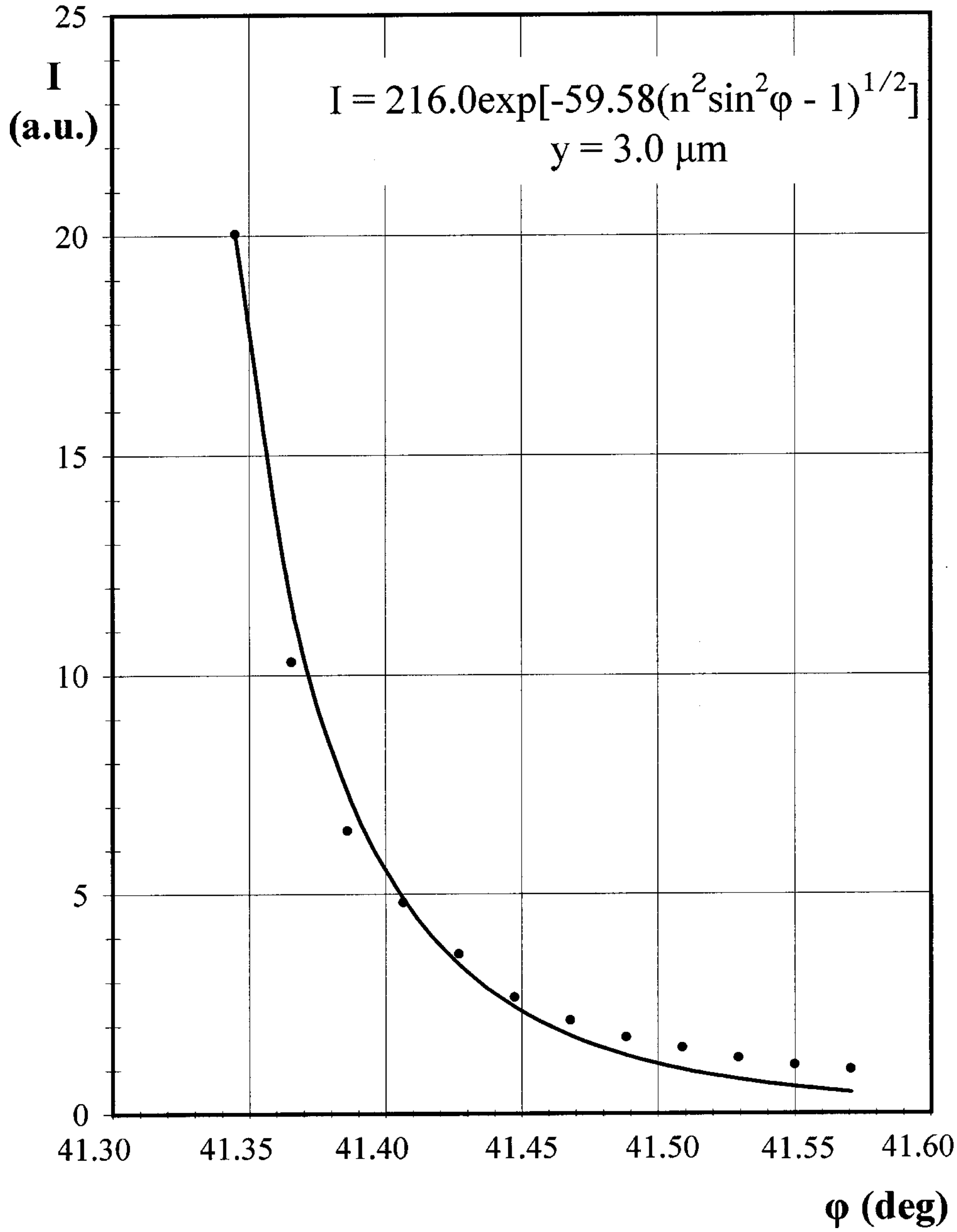

Fig. 6. Intensity vs angle of incidence for a constant probe-to-surface distance. Other details are the same as in Fig. 3.

assumption that the exponential term in Eq. (3) contains all of the changes in the intensity through the dependence of the penetration depth on the angle of incidence. This assumption becomes worse as the angle of incidence departs further from the critical angle, and may in part explain the slight deviation seen in the right part of the figure. To examine this point further, the variation in $|\mathbf{A}|^2$ with the angle of incidence would have to be taken into account, which, for the present purpose, would complicate the issue unnecessarily.

In the final experiment the probe was held at a fixed distance $y \approx 3.00\ \mu$m while the angle of incidence was varied to estimate the dependence $I(\varphi)$. The results are shown in Fig. 6 together with a theoretical fit based on Eq. (3), again with the assumption that all variations can be attributed to the exponential term for small excursions from the critical angle of incidence. To realize these measurements the axis of rotation of the microscope stage has to coincide exactly with the tip of the probe to maintain a constant probe-to-surface distance. This requirement was not easy to do with our equipment and the measured data seem to suffer as a result.

V. CONCLUSIONS

We have presented an experimental method that allows one to directly observe the presence of an evanescent wave. The technique relies on the observation of light scattered by a metallic probe in close proximity to the surface where the evanescent wave is produced by total internal reflection. As only low-cost components are used, the method is highly suitable for educational purposes and, with minor additional efforts, it can be used to examine the properties of evanescent waves in more detail. We have found that for only small excursions from the critical angle of incidence, the experimental results compare reasonably well with a simple theoretical model where the probe is considered to be a local and passive intensity detector of the evanescent wave field. More accurate approaches are available, but they would require a much more rigorous treatment of both the probe and the probe–surface interaction,[15] and although they would definitively increase the accuracy of our comparison, they would hinder the straightforward appeal of the present study.

ACKNOWLEDGMENTS

The authors wish to thank D. A. Petsoris and V. A. Poulou, graduate students in physics, for their assistance during measurements and data reduction.

[a]Electronic mail: dpapatha@phys.uoa.gr

[1]I. Newton, *Opticks* (Dover, New York, 1952), Book two, Part I.
[2]G. Quincke, ‘‘Ueber das Eindringen des total reflectirten Lichtes in das dünnere Medium,’’ Ann. Phys. (Leipzig) **127**, 1–29 (1866).
[3]J. C. Bose, ‘‘On the influence of the thickness of air-space on total reflection of electric radiation,’’ Proc. R. Soc. London **62**, 300–310 (1897).
[4]E. E. Hall, ‘‘The penetration of totally reflected light into the rarer medium,’’ Phys. Rev. **15**, 73–106 (1902).
[5]S. Zhu, A. W. Yu, D. Hawley, and R. Roy, ‘‘Frustrated total internal reflection: A demonstration and review,’’ Am. J. Phys. **54**, 601–607 (1986).
[6]R. Weigand and J. M. Guerra, ‘‘Demonstration of the evanescent wave through absorption,’’ Am. J. Phys. **64**, 913–916 (1996).
[7]F. Albiol, S. Navas, and M. V. Andres, ‘‘Microwave experiments on electromagnetic evanescent waves and tunneling effect,’’ Am. J. Phys. **61**, 165–169 (1993).
[8]J. M. Vigoureux, C. Girard, and D. Courjon, ‘‘General principles of scanning tunneling optical microscopy,’’ Opt. Lett. **14**, 1039–1041 (1989).
[9]L. Salomon, F. de Fornel, and J. P. Goudonnet, ‘‘Sample-tip coupling efficiencies of the photon-scanning tunneling microscope,’’ J. Opt. Soc. Am. A **8**, 2009–2015 (1991).
[10]F. de Fornel, *Evanescent Waves* (Springer, Heidelberg, 2001).
[11]B. A. E. Saleh and M. C. Teich, *Fundamentals of Photonics* (Wiley-Interscience, New York, 1991).
[12]M. V. Klein and T. E. Furtak, *Optics* (Wiley, New York, 1986), pp. 84–85.
[13]B. Vohnsen and S. I. Bozhevolnyi, ‘‘Optical characterization of probes for photon scanning tunnelling microscopy,’’ J. Microsc. **194**, 311–316 (1999).
[14]J. C. Weeber, F. de Fornel, and J. P. Goudonnet, ‘‘Numerical study of the tip-sample interaction in the photon scanning tunneling microscope,’’ Opt. Commun. **126**, 285–292 (1996).
[15]C. Girard and A. Dereux, ‘‘Near-field optics theories,’’ Rep. Prog. Phys. **59**, 657–699 (1996).

D-DAY AND RADAR

Under the stormy skies of D-Day itself, the Rad Lab's state-of-the-art radar systems stood watch, guaranteeing the Allied troops fire support during the landing and security from surveillance. On June 6, 1944, the largest amphibious invasion force ever mounted hit the beaches at Normandy. They were accompanied by a total of thirty-nine SCR-584 radar sets, which would help protect the infantry from air attacks as they advanced through Europe. In the darkness of the early morning hours, 450 airplanes equipped with H2X radar systems bombarded the French coastline, cloaking the beach in clouds of smoke and dust as five Allied divisions—two American, two British, and one Canadian—struggled ashore through the surf and dodged enemy fire as they headed for the shelter of the cliffs. It was a precisely timed operation, allowing only five minutes between when the last bomb fell and the first swarm of infantry debarked. While no Allied troops were felled by misdirected bombs, the fear of releasing payloads on their own men compounded a variety of other errors, resulting in hundreds of bombs being dropped onto fields behind German front lines and leaving thousands of American soldiers to be slaughtered at the water's edge on Omaha beach. The air bombardment was more successful at Utah beach, where radar beacons successfully guided parachute troops and glider-borne infantry to their targeted drop zones. The Rad Lab's precise navigation system, known as landing craft control (LCC), was also used to control the landing of the invasion force, directing wave after wave of assault troops to prearranged points on the sixty-mile-long beach.

Jennett Conant, *Tuxedo Park* (Simon & Schuster, New York, NY, 2002), p. 270.